

1 How marine currents and environment shape  
2 plankton genomic differentiation: a mosaic view  
3 from *Tara* Oceans metagenomic data

4 Romuald Laso-Jadart<sup>1,4\*</sup>, Michael O'Malley<sup>2</sup>, Adam M. Sykulski<sup>2</sup>, Christophe Ambroise<sup>3</sup>, Mohammed-  
5 Amin Madoui<sup>1,4\*</sup>

6 <sup>1</sup>Génomique Métabolique, Genoscope, Institut François Jacob, CEA, CNRS, Univ Evry, Université Paris-  
7 Saclay, Evry, France.

8 <sup>2</sup>STOR-i Centre for Doctoral Training/Department of Mathematics and Statistics, Lancaster University,  
9 UK

10 <sup>3</sup>LaMME, CNRS, Univ Evry, Université Paris-Saclay, Evry, France

11 <sup>4</sup>Research Federation for the study of Global Ocean Systems Ecology and Evolution, FR2022/Tara  
12 Oceans GO-SEE, 3 rue Michel-Ange, 75016 Paris, France

13 \* Corresponding authors. Emails: [rlasojad@genoscope.cns.fr](mailto:rlasojad@genoscope.cns.fr) & [amadoui@genoscope.cns.fr](mailto:amadoui@genoscope.cns.fr)

## 14 **Abstract**

15 Plankton seascape genomics show different trends from large-scale weak differentiation to micro-scale  
16 structures. Prior studies underlined the influence of environment and seascape on a few single species  
17 differentiation and adaptation. However, these works generally focused on few single species, sparse  
18 molecular markers, or local scales. Here, we investigate the genomic differentiation of plankton at macro-  
19 scale in a holistic approach using *Tara* Oceans metagenomic data together with a reference-free  
20 computational method to reconstruct the  $F_{ST}$ -based genomic differentiation of 113 marine planktonic  
21 species using metavariant species (MVS). These MVSs, modelling the species only by their  
22 polymorphism, include a wide range of taxonomic groups comprising notably 46 Maxillopoda/Copepoda,  
23 24 Bacteria, 5 Dinoflagellates, 4 Haptophytes, 3 Cnidarians, 3 Mamiellales, 2 Ciliates, 1 Collodaria, 1  
24 Echinoidea, 1 Pelagomonadaceae, 1 Cryptophyta and 1 Virus. The analyses showed that differentiation  
25 between populations was significantly lower within basins and higher in bacteria and unicellular  
26 eukaryotes compared to zooplankton. By partitioning the variance of pairwise- $F_{ST}$  matrices, we found that  
27 the main drivers of genomic differentiation were Lagrangian travel time, salinity and temperature.  
28 Furthermore, we classified MVSs into parameter-driven groups and showed that taxonomy poorly  
29 determines which environmental factor drives genomic differentiation. This holistic approach of plankton  
30 genomic differentiation for large geographic scales, a wide range of taxa and different oceanic basins,  
31 offers a systematic framework to analyse population genomics of non-model and undocumented marine  
32 organisms.

## 33 Introduction

34 Marine species from epipelagic plankton are drifting organisms abundantly present in every ocean,  
35 playing an active role in Earth biogeochemical cycles (1,2) □ and form a complex trophic web (3,4) of  
36 high taxonomic diversity (5–7) at the basis of fish resources (8,9)□. Understanding the present  
37 connectivity between populations or communities of plankton is thus crucial to apprehend upheavals due  
38 to climate change consequences in oceans (10,11)□.

39 Due to their potential high dispersal and huge population size, planktonic species have long been thought  
40 to be homogenous and highly connected across oceans, but this assumption is challenged by empirical  
41 studies since two decades (12)□. Planktonic species are characterized by theoretical high population  
42 effective sizes (13,14)□, which reduces the power of drift and makes selection and beneficial mutation  
43 stronger drivers of their evolution, as exemplified in the SAR11 alphaproteobacteria (15)□, but the balance  
44 between neutral evolution and selection is still debated (16,17)□. Furthermore, evolution in plankton also  
45 seems to be strengthened by acclimation through variation of gene expression or changing phenotypes in  
46 response to environmental conditions (18–21)□.

47 Gene flow and connectivity between planktonic populations can be impacted by three major forces:  
48 marine currents, abiotic (i.e physico-chemical parameters) and biotic factors. First, as planktonic species  
49 are passively and continuously transported by marine currents, we could expect that isolation-by-distance  
50 shapes the genetic structure of populations. Conversely, cosmopolitan, panmictic and/or unstructured  
51 species have been reported multiple times in Copepoda (21–24)□, Collodaria (25)□ or Cnidaria (26).  
52 Other studies show more complex patterns, with genetic structure mainly observed at the level of basins in  
53 Copepoda (27)□, Pteropoda (28)□, Diatoms (29)□ and Cnidaria (30) or at mesoscale in Chaetognatha  
54 (31)□, Copepoda (32–34)□, Dinophyceae (35) or *Macrocystis pyrifera* (36)□. Thus, due to the  
55 complexity of oceanic processes, classical landscape genomics frameworks began to be applied and  
56 adapted (37) to better model the dispersion of populations over seascape, or what we would call

57 “isolation-by-currents”. Hence, modelling oceanic circulation at macro- and meso-scale is a prerequisite to  
58 capture the water masses connectivity (38)□. Successful approaches using data derived from larval  
59 dispersal models were used in fish and coral (39–41)□ and the relatively recent use of Lagrangian travel  
60 time estimates combined with genetic data showed promising results (34,36) to better explain gene flow □.

61 At the same time, changing environmental conditions may lead to selective pressure that counter the effect  
62 of dispersion induced by marine currents, leading to a higher differentiation. The best examples are  
63 temperature-driven structures from bacteria to cnidaria (15,30)□ or the effect of salinity in diatoms (42)□,  
64 that can even favours speciation in estuaries (43)□. Finally, biotic drivers based on competition and co-  
65 evolution were also reported to shape evolution (44)□. However, abiotic and biotic parameters are often  
66 linked to oceanic circulation, which leads to technical challenge to disentangle the role and importance of  
67 each parameter on populations’ connectivity.

68 All these above mentioned findings usefully enhanced our understanding of plankton connectivity, like in  
69 zooplankton (45)□, but they focused on documented species with reference sequences, often using few  
70 molecular markers such as mitochondrial (COI) or ribosomal genes (16S, 18S, 28S), and/or are restricted  
71 to mesoscale sampling. Thus, we need to overcome these case studies by adopting a holistic approach  
72 which integrates the analyses of genome-wide markers belonging to species from different levels of the  
73 trophic chain, sampled across the world oceans.

74 Advances in environmental genomics realized by shotgun sequencing offer a new perspective for  
75 population genomics of marine plankton species based on metagenomic data. Diversity in ocean  
76 microorganisms can now be better understood, thanks to ambitious expeditions (46,47). Particularly, *Tara*  
77 Oceans data provide a unique dataset from many locations in all the world oceans, enabling global  
78 approaches to investigate plankton (7,48–51), but blind spots in term of taxonomy or function are still an  
79 obstacle for further analyses, due to the lack of reference genomes or transcriptomes. The first way to  
80 address this issue relies on the use of the metagenome-assembled genomes (MAGs) from metagenomic  
81 data that enable to retrieve a large amount of lineages from metagenomic samples, especially for small-

82 sized genomes as found in viruses and prokaryotes (48,52–55). A second way is the single-cell sequencing  
83 after flow-cytometric sorting (56) which allows the genome reconstruction of small eukaryotic species.  
84 Both ways increase the number of available references. An alternative way is based on a reference-free  
85 approach of metagenomic data (57), in order to analyse the population differentiation of numerous  
86 unknown species potentially lacking a reference.

87 Here, we proposed to study plankton connectivity from a holistic point of view, using metagenomic data  
88 extracted from samples gathered during *Tara* Oceans expeditions in Mediterranean Sea, Atlantic and  
89 Southern Oceans. After extracting polymorphic data and clustering them into metavariant species (MVS)  
90 using a reference-free method (57), we coupled environmental parameters and a new modelling of  
91 Lagrangian travel times (58) to estimate the relative contribution of environment and marine currents on  
92 the population differentiation of these MVSs.

## 93 **Material and Methods**

### 94 **Extracting metavariants from *Tara* Oceans metagenomic data**

95 Metavariants are nucleotidic variants detected directly from metagenomic data using the reference-free  
96 variant caller *DiscoSNP++* (59) with parameters `-k 51 -b 1`(60) (Arif et al. 2018)□. We used a set of  
97  $23 \times 10^6$  metavariants produced in a previous study (60)□. These metavariants were detected in 35 *Tara*  
98 Oceans sampling sites corresponding to four distinct size fractions (0.8-5  $\mu\text{m}$ , 5-20  $\mu\text{m}$ , 20-180  $\mu\text{m}$  and  
99 180-2000  $\mu\text{m}$ ) from the water surface layer, for a total of 114 samples (Figure 1A). For further analyses,  
100 *Tara* stations were separated into four groups corresponding to the basins they belong to: the  
101 Mediterranean Sea (MED; TARA\_7 to TARA\_30), Northern Atlantic Ocean (NAO; TARA\_4,  
102 TARA\_142 to TARA\_152), Southern Atlantic Ocean (SAO; TARA\_66 to TARA\_81), and Southern  
103 Ocean (SO; TARA\_82 to TARA\_85). Full protocols for sampling, extractions and sequencing are detailed  
104 in previous studies (61,62).

## 105 **Construction of metavariant species**

106 To identify sets of loci belonging to unique species, we used metaVaR version v0.2 (57). This method  
107 enables the clustering by species of metavariants previously called from metagenomic raw data. Each  
108 cluster is constituted of genomic variants of a single species and the final clusters are called metavariant  
109 species (MVSs).

110 The metavariants of the four size fractions were filtered using metaVarFilter.pl with parameters -a 5 -b  
111 5000 -c 4. This process discarded low covered loci, repeated regions that present very high coverage and  
112 loci with non-null coverage in less than four samples.

113 The second step of the metaVaR process clusters the metavariants. MetaVaR uses multiple density-based  
114 clustering (dbscan, (63,64)□), a total of 187 couples of parameters epsilon and minimum points ( $\epsilon$ ,  
115 MinPts) were tested, with  $\epsilon = \{4,5,6,7,8,9,10,12,15,18,20\}$  and MinPts  
116  $= \{1,2,3,4,5,6,7,8,9,10,20,50,100,200,300,400,500\}$ . This clustering phase constitutes a set of clusters  
117 called metavariant clusters (MVC) for each couple (Supplementary Figure S1). Then a maximum  
118 weighted independent sets (MWIS) algorithm was used on the resulting set of MVCs to select the best  
119 non-overlapping clusters, i.e. clusters sharing no metavariants. For the dataset corresponding to the size  
120 fraction 20-180 $\mu$ m, 220 MVCs containing more than 90% of the metavariants were discarded to decrease  
121 the memory use during the MWIS computation. For each selected MWIS, only loci with a depth of  
122 coverage higher than 8x were kept. Finally, only MVSs with at least 100 variants, and for which at least  
123 three samples presented a median depth of coverage  $> 8x$  were retained, leading to a final set of 113  
124 MVSs. As a result, metaVaR provides a frequency matrix and a coverage matrix across each biallelic  
125 locus in each population for each MVS that will be used further for population genomic analyses.

## 126 **Taxonomic assignment of MVSs**

127 To provide a taxonomic assignment of each MVS, three different assignments were performed, using  
128 different sources of information (Supplementary Figure S2).

129 First, for each size fraction, the sequences supporting the metavariants were mapped on downloaded  
130 NCBI non-redundant database (10/23/2019) with diamond v0.9.24.125 (65)□, using blastx and parameter  
131 -k 10, and the results were filtered based on the E-value ( $<10^{-5}$ ). Then, for each variant, the taxonomic ID  
132 and bitscore of each match were kept. A fuzzy Lowest Common Ancestor (LCA) method (66) was used to  
133 assign a taxonomy to each sequence, using bitscore as a weight with -r 0.67 -ftdp options. The highest  
134 phylogenetic ranks were retained as the best assignation for each sequence. This constituted a first  
135 taxonomic assignation of the metavariant sequences. In parallel, the sequences were mapped on MATOU,  
136 a unigen catalog based on *Tara* Oceans metatranscriptomic data (50)□, and on the MMETSP  
137 transcriptomic database (67)□. This constituted three different taxonomic assignations of the variant  
138 sequences.

139 Then, for each MVS, the unfiltered variant sequences from the corresponding MVC were used to  
140 maximize information. The three mentioned taxonomic assignations were crossed with the MVC  
141 sequences and the sequences assigned to the same clade were summed and used as a basis for a manual  
142 taxonomic assignation of the MVS. Each MVS was thus assigned to the most probable taxonomic clade.  
143 MVSs were then regrouped into 24 taxonomic groups that were clustered into six reliable wider groups:  
144 Virus, Bacteria, Unicellular Eukaryotes, Animals, Copepods, and Poor classification (Figure 2B). This  
145 offered three levels of assignation, from the most precise to the widest (Supplementary Table S1).

#### 146 **Population genomics analysis**

147 To investigate genomic differentiation at different scales, the  $F_{ST}$  metrics was used throughout this study  
148 and computed for each variant of an MVS as follows,  $F_{STi} = \frac{\sigma_i^2}{\bar{p}_i(1-\bar{p}_i)}$ , with  $\bar{p}_i$  and  $\sigma_i^2$  being respectively the  
149 mean and variance of allele frequency across the considered populations  $i$  (68)□. Two types of  
150 computations were launched, in each MVS. A first global  $F_{ST}$  was calculated using the total set of  
151 populations, allowing the analysis of the global  $F_{ST}$  distribution. Then, a pairwise- $F_{ST}$  was calculated  
152 between the populations, and median pairwise- $F_{ST}$  was retained as a measure of genomic differentiation  
153 between the populations of the MVS.

154 For the whole set of MVSs, each pairwise- $F_{ST}$  comparison was extracted from the metaVaR outputs.  
155 These pairwise- $F_{ST}$  were compared in three different statistical frameworks, by grouping them based on  
156 the following factors: the basins where the two populations are located, the taxonomic assignation of the  
157 MVS and the size fraction of the MVS. For each comparison, a Kruskal-Wallis test was used to assess the  
158 significance of the variation of the median pairwise- $F_{ST}$  among groups. When the test was significant ( $p$ -  
159 value  $<0.05$ ), multiple comparison Wilcoxon tests were performed between groups.

### 160 **Connection within and between basins**

161 To estimate the connection between and within basins, we regrouped *Tara* stations based on their  
162 locations (i.e. MED, NAO, SAO and SO), and computed the mean  $F_{ST}$  between and within basins. As an  
163 example, if we compared MED to SO, we extracted, from the median pairwise- $F_{ST}$  matrices of all MVSs,  
164 all the median pairwise- $F_{ST}$  between a MED station and an SO station were compared, and kept the mean  
165 of this distribution as an estimate of differentiation.

### 166 **Lagrangian travel time estimation**

167 To estimate Lagrangian transport, we used a method based on drifter data (58)□. The method is used to  
168 compute the travel time of the most likely path between *Tara* stations, back and forth. We used the public  
169 database of the Global Drifter Program (GDP), managed by the National Oceanographic and Atmospheric  
170 Administration (NOAA) (<https://www.aoml.noaa.gov/phod/gdp/>) containing information from drifters  
171 ranging from February 15, 1979 to September 31, 2019. We extracted the data for both drogued and  
172 undrogued drifters (i.e. drifters that lost their sock) to maximize the information used by the method. No  
173 drifters have ever been observed to get out of the Mediterranean Sea through the Strait of Gibraltar,  
174 therefore to avoid missing data, we arbitrarily added 100 years to the travel times of pathways out of the  
175 Mediterranean Sea over the Strait of Gibraltar and added 1 year to the pathways going into the  
176 Mediterranean Sea, based on previous models on surface water (69,70)□. We used 450 rotations within  
177 the method to reduce the reliance of travel times on the grid system used. Two travel times are obtained by  
178 the method for each pair of stations: back and forth, resulting in an asymmetric travel time matrix between



179 all possible station pairings. For our analyses, we retained only the minimum of these two travel times in  
180 the matrix, as this then accounts for the direction of currents between stations.

### 181 **Environmental data**

182 Environmental variables corresponding to the 35 selected *Tara* stations were extracted from the World  
183 Ocean Atlas public database (<https://www.nodc.noaa.gov/OC5/woa13/woa13data.html>), for the period  
184 2006-2013 on  $1^\circ \times 1^\circ$  grid, covering the dates of *Tara* Oceans expeditions. The following parameters were  
185 retrieved: temperature ( $^\circ\text{C}$ ), salinity (unitless), silicate ( $\mu\text{mol.L}^{-1}$ ), phosphate ( $\mu\text{mol.L}^{-1}$ ) and nitrate  
186 ( $\mu\text{mol.L}^{-1}$ ).

### 187 **Variation partitioning of the genomic differentiation of MVSs**

188 To estimate the relative contribution of environmental parameters and Lagrangian travel time in the  
189 variance of each MVS genomic differentiation, a linear mix model (LMM) was applied with R package  
190 MM4LMM (71). The model applied was the following;  $Y_{FST} = \mu + Zu + \varepsilon$ , where  $Y_{FST}$  is the vector of  
191 observations of  $F_{ST}$  values with a mean  $\mu$ ,  $Z$  is a known matrix of parameters relating the observations  $Y_{FST}$   
192 to  $u$ , a vector of independent random effects of zero mean and  $\varepsilon$  is a vector of random errors of 0 means  
193 and covariance matrix proportional to the identity (white noise).

194 For each pairwise- $F_{ST}$  matrix, the corresponding matrix of minimum Lagrangian travel time was retrieved.  
195 Temperature, salinity, silicate, phosphate and nitrate measures were extracted for all the stations where the  
196 MVS is present, and a Euclidean distance was computed between the stations for each of these  
197 parameters. The LMM was then applied on pairwise- $F_{ST}$  values using the five environmental distances  
198 and Lagrangian travel time after scaling, adding a variance of 1 for each explicative variable. To note, we  
199 considered the parameters as independent variables. As a result, an estimate of the contribution of each  
200 parameter to the total variance of pairwise- $F_{ST}$  is obtained. In addition, a fixed effect and a proportion of  
201 variance unexplained (corresponding to the noise) is retrieved.

202 In order to investigate the structure of the MVSs relative to their  $F_{ST}$  variance decomposition, two

203 principal component analyses (PCA) were then performed. A first one was done on the variance explained  
204 by the six variables and the unexplained part of the variance over the 113 MVSs. From this PCA, the  
205 unexplained variance of  $F_{ST}$  (Supplementary Figure S4) was high in most of MVSs, strongly contributing  
206 to the first component (37% explained variance). For clarity, a second PCA was conducted by removing  
207 the unexplained part of the variance. For both PCAs, correlation of the variables with the components and  
208 the contribution (i.e. the ratio of the  $\cos^2$  of each variable on the total  $\cos^2$  of the components) of the  
209 variables to the components were extracted. PCAs were performed using FactoMineR v2.3 R package  
210 (72,73)□.

### 211 **Clustering MVSs into specific parameters-driven differentiation groups**

212 The variance explained by each factor was used to represent the MVSs with dimensional reduction  
213 through t-distributed Stochastic Neighbor Embedding (t-SNE), using Rtsne R package (74) with a  
214 perplexity of 5 and 5,000 iterations and we extracted the MVS coordinates. Then, a k-means clustering ( $K$   
215 = 8) was performed to identify MVSs with common patterns of explained variance. To identify which set  
216 of parameters drives the differentiation of a cluster, we compared the distributions of the explained  
217 variance of each parameter within the cluster using a Kruskal-Wallis and a Wilcoxon paired tests (p-value  
218 < 0.05).

## 219 **Results**

### 220 **Taxonomy and biogeography of MVSs**

221 We used  $23 \times 10^6$  metavariants generated from 114 metagenomics data of 35 *Tara* samples with  
222 *DiscoSNP++* in a previous study (60) as input for metaVaR and we constructed a total of 113 MVS out of  
223 4,220 MVCs (Figure 1B, Supplementary Table S1), containing altogether 68,575 metavariants (0.3% of  
224 the total, Figure 1B). The taxonomic assignation of the MVS showed a wide range of lineages spanning  
225 all the plankton trophic levels, with a predominance of Maxillopoda/Copepoda (46), Bacteria (24) and  
226 Eumetazoa (21, comprising three Cnidaria and one Echinodea) (Figure 2B). In Bacteria, we found 9

227 Cyanobacteria, with 8 MVSs linked to *Synechococcus* and one to *Prochlorococcus*. Other notable  
228 eukaryotic species belonged to Dinophyceae (5), Haptophyta (4), Mamiellales (3), Collodaria (2),  
229 Ciliophora (2), Cryptophyta (1) and Pelagomonadacea (1). Only four MVSs presented a poor assignment  
230 (unclassified or Eukaryotes) and one MVS was a virus. In Mamiellales, two MVSs were identified as  
231 *Bathycoccusprasinus* and are related to previously observed results from *Tara* Oceans (Supplementary  
232 Table S2). The size of MVSs ranged from 114 to 1,767 variants and was unrelated to the size fraction  
233 (Figure 1A, Kruskal-Wallis p-value > 0.05). As expected, bacteria dominate smaller size fractions, and  
234 Eumetazoa (Cnidaria, Bilateria, Copepods) are found in higher size fractions.

235 A vast majority of MVSs (95, 84%) were present in four to six stations, with a maximum of eight stations  
236 for an MVS (Supplementary Figure S5). The number of MVSs per stations showed an important variation  
237 (Figure 2D), from four to 43 MVSs (TARA\_67/81/84/85 and TARA\_150 respectively). Notably, stations  
238 from Southern Ocean (TARA\_82 to 85) contained few MVSs compared to the others (from 4 to 7 MVSs),  
239 with four MVSs (Gammaproteobacteria, Haptophyta, Flavobacteriia and Calanoida) being solely present  
240 in Southern Ocean (SO). Finally, 36 MVSs were present in only one basin, while a majority of MVSs (80)  
241 were present in Northern Atlantic Ocean (NAO) and in one other basin (Figure 2C).

#### 242 **Global view of MVSs genomic differentiation**

243 Pairwise- $F_{ST}$  was used to estimate the population differentiation among the MVSs. First, we saw that  
244 differentiation between populations was significantly more important among basins than within basins  
245 (Figure 3A), for each size fraction separately or together. When we compared the basins (Figure 3B),  
246 NAO presented weak differentiation with MED and SAO (0.118 and 0.143 respectively). SAO and MED  
247 presented a relatively higher differentiation between them (0.222). Finally, this analysis underlined the  
248 important global differentiation of the SO from other basins (0.201-0.555), but also a high differentiation  
249 within the SO (0.397).

250 Secondly, population differentiation was significantly different between size fractions (Kruskal-Wallis, p-  
251 value < 0.05), being higher in 0.8-5 $\mu$ m and lower in 180-2000 $\mu$ m (Figure 3C). Population differentiation

252 between the six larger taxonomic groups (see Methods) was related to the body size of the lineages, with a  
253 differentiation being relatively lower in copepods and other animals than in unicellular eukaryotes,  
254 bacteria and virus (Figure 3D).

255 We observed a large spectrum of population genomic differentiation patterns among MVSs (Figure 3E),  
256 with maximum median pairwise- $F_{ST}$  between 0.03 and 1. Extreme cases were observed, for 13 MVSs  
257 presenting one or more populations with a median pairwise- $F_{ST}$  of 1, and a global  $F_{ST}$  distribution strongly  
258 shifted to 1, as exemplified by the Collodaria (MVS 15\_200\_2, Supplementary Figure S6). We then saw that  
259 the number of basins where MVSs were spotted was not significantly linked to their global  $F_{ST}$  (Kruskal-  
260 Wallis p-value > 0.05, Figure 3F).

#### 261 **Computing Lagrangian estimates of marine travel times**

262 Based on recorded drifter motion throughout the ocean, we computed Lagrangian travel time estimates  
263 between the 35 *Tara* stations, and observed three clear patterns, distinguishing the MED, NAO and  
264 SAO/SO (Figure 4A, Supplementary Figure S7). These results also showed interesting cases illustrated by  
265 the following four examples: (i) the relative proximity from TARA\_66 to 76 (SAO) and to other NAO  
266 stations, (ii) the link from SO stations to TARA\_66 and 70, despite a large geographic distance, (iii) the  
267 isolation from TARA\_145 to the rest of NAO stations, (iv) a separation from TARA\_7/9/11 to the rest of  
268 MED stations.

#### 269 **Estimating the relative role of environment and marine currents**

270 To estimate the relative role of environmental factors and marine currents in the genomic differentiation of  
271 plankton, we first extracted the data from World Ocean Atlas (Figure 4B) for temperature, salinity, nitrate,  
272 silicate and phosphate. Then, we modelled pairwise- $F_{ST}$  of each MVS as the variable depending on the  
273 five environmental and Lagrangian times variables using a linear mixed model (LMM). The fixed part of  
274 the explained variance was low for each MVS, ranging from 0 to 14% (Supplementary Table S1), and was  
275 not further analysed. Among all tested environmental variables, Lagrangian travel time, temperature and  
276 salinity were the major contributors to the genomic differentiation (Figure 5A), highly correlated to the

277 three first components (67% explained variance). The variance contribution of nitrate, silicate and  
278 phosphate respectively followed on the last three components.

279 MVSs were then clustered into eight groups by k-means, based on their t-SNE coordinates (Figure 5B).  
280 Then, we identified the most important variables over the MVSs of each cluster (Figure 5C), to  
281 characterize the clusters. Two clusters were linked to Lagrangian travel times, labelled as “Lagrangian”  
282 (14 MVSs) and “Lagrangian 2” (13), the latter exhibiting a lower explained variance by Lagrangian. The  
283 largest cluster contained 24 MVSs but was not linked to any parameter. The others are linked to a single  
284 environmental parameter: salinity (16 MVSs), temperature (14), silicate (13), phosphate (13) and nitrate  
285 (10).

286 More precisely, the clusters “Lagrangian”, “Temperature” and “Salinity” presented clear differences  
287 between their respective drivers compared to the other parameters (Figure 5C). The clusters “Phosphate”  
288 and “Silicate” showed a wider distribution of their respective driver among the MVSs they contained, with  
289 respectively salinity and phosphate sharing high proportion of explained variance. The “Nitrate” cluster  
290 also regrouped MVSs for which a non-negligible part of variance was explained by Lagrangian travel  
291 time.

292 Each cluster showed MVS assigned to almost all taxonomic groups and presented no particular visual  
293 enrichment (Figure 5C). This absence of enrichment is clearer in copepods, which constitute the majority  
294 of MVSs (Fisher’s Exact Test p-value = 0.348).

295 Among the nine MVSs belonging to the “Lagrangian” cluster, we observed five MVSs present in  
296 Mediterranean Sea and Southern Atlantic and one in Northern and Southern Atlantic. Interestingly, two  
297 MVSs were restrained to a single basin, respectively Southern Ocean and Northern Atlantic. Notably, the  
298 latter, Planctomycetales 9\_200\_1, shows a differentiation linked to local marine barriers, with TARA\_148  
299 being isolated from the others, TARA\_150 and 151 being closely related, and TARA\_152 connected to  
300 the others, but with slightly higher values (Figure 6A).

301 Another example one of within-basin differentiation concerns the Mediterranean gammaproteobacteria  
302 7\_300\_4 from the “Lagrangian 2” cluster, for which the differentiation clearly shows a pattern linked to  
303 marine currents (Figure 6B), with a clear separation between TARA\_7, 9 and TARA\_23, 25, and  
304 TARA\_18 being genetically closer to TARA\_9, this is explained by Lagrangian estimates together with a  
305 small contribution of salinity.

306 Some MVSs displayed a clear link between their differentiation and one environmental parameter. For  
307 example, in the “Phosphate” cluster, we found a Dinophyceae MVS (8\_10\_11), that displayed a clear  
308 unimodal  $F_{ST}$  distribution and no structure between NAO and SAO (Figure 6C). For this Dinophyceae, the  
309 population of TARA\_70 seemed more isolated to the other NAO populations and TARA\_70 is  
310 characterized by a higher phosphate concentration ( $0.264 \mu\text{mol.L}^{-1}$  against  $0.031\text{-}0.106 \mu\text{mol.L}^{-1}$ ).

311 Inside the “Nitrate” cluster, there is an example of one Mamiellale MVS (5\_100\_1) for which populations  
312 from TARA\_146 and TARA\_147 were highly connected, and TARA\_142 was more connected to  
313 TARA\_146 than TARA\_147. This reflects the differences in nitrate between these locations (Figure 6D).

314 In the “Temperature” cluster, the cosmopolitan Calanoida MVS 12\_5\_104, detected in the MED, NAO  
315 and SAO (Figure 6E), presented a relatively higher genetic distance between populations from TARA\_20  
316 and 68 ( $F_{ST} = 0.08$ ). This genetic pattern was linked to a higher difference in temperature of  $5.2^{\circ}\text{C}$  with  
317 respectively  $21.9^{\circ}\text{C}$  and  $16.7^{\circ}\text{C}$ .

318 In the “Silicate” cluster, we have an illustration of a differentiation along a gradient of silicate, in the  
319 cyanobacteria 8\_100\_13, showing a high isolation of the TARA\_151 population compared to populations  
320 from TARA\_146, 147 and 150 (Figure 6F). The genetic isolation of TARA\_151 was linked to a higher  
321 concentration in silicate in Northern East Atlantic.

322 We also found MVSs belonging to a cluster but showing another parameter that also explained a great  
323 proportion of the genomic differentiation. As an example, we found the Cnidaria 20\_100\_10 from the  
324 “Salinity” cluster, for which temperature was also an important explaining factor (Figure 6G). Also, the

325 Cyanobacteria 7\_7\_9 from “Lagrangian 2” cluster presented a clear differentiation between MED and  
326 NAO (Figure 6H), which was explained by both Lagrangian travel times and salinity, the Mediterranean  
327 Sea presenting higher salinity than NAO.

### 328 **Focus on Antarctic genomic differentiation of plankton**

329 From the analysis of global  $F_{ST}$ , it seemed SO presented a pattern of relative isolation from the other  
330 basins (Figure 3B). Indeed, we observed that the same four MVSs (Gammaproteobacteria 12\_100\_16,  
331 Flavobacteriia 7\_100\_6, Haptophyta 4\_50\_2 and Calanoida 5\_20\_1) can be found in stations TARA\_82,  
332 83, 84 and 85 from the SO. Furthermore, using Lagrangian trajectories (Supplementary Figure S8), the  
333 two main currents of the area were spotted: the Malvinas Current and The Antarctic Circumpolar Current  
334 (ACC) (Figure 7A). These MVSs presented among the highest global median  $F_{ST}$  (0.35 to 0.84, see  
335 Supplementary Figure S6), revealed a very high differentiation between their populations (Figure 7B), and  
336 all belonged to different clusters (“Salinity”, ”Unknown”, ”Lagrangian” and ”Nitrate” respectively).  
337 Particularly, the Haptophyta MVS presents a differentiation linked to both the ACC and the Malvinas  
338 Current.

## 339 **Discussion**

### 340 **Metavariant species as a representation of species polymorphism**

341  
342 Metavariant species were detected in each of the four size fractions. The number of genomic variants  
343 varied from 114 to several hundreds, with a very low rate of estimated false positive metavariants (46)  
344 enabling a realistic overview of the population structures of marine planktonic species lacking reference  
345 sequences. With this approach, metagenomic data help us to draw the silhouette of species population  
346 structure while previous studies are often based on few genetic markers, few samples, and are restrained to  
347 small geographic areas.

348 We were able to detect an extensive range of taxa, reflecting the biodiversity of epipelagic layer of oceans.  
349 It must be noticed that for each MVS, a majority of variant sequences didn't show any taxonomic signal,  
350 an observation already made in other studies using *Tara* Oceans data (50,51). The level and quality of  
351 taxonomical assignation are both due to a lack of references in databases and to the small size of the  
352 sequences, reducing the chance of matching a reference and having a clear assignation.

353 Notwithstanding these technical limits for the taxonomical annotation of the MVS, four notable taxonomic  
354 groups retrieved from MVSs can be described and be related to previous observations. First, we were able  
355 to detect a virus, from the order of Caudovirales, and probably belonging to the bacteriophage family of  
356 Myoviridae. These viruses are known to be abundant compared to other viruses in oceans (75)□, notably  
357 infecting Cyanobacteria (i.e. *Prochlorococcus* and *Synechococcus*), and constitute the majority of viral  
358 populations in GOV 2.0 (76)□. Second, two Cyanobacteria, probably two *Synechococcus* (15\_500\_9 and  
359 7\_20\_37) were detected in the same locations in Mediterranean Sea, with clear  $F_{ST}$  unimodal distributions  
360 (Supplementary Figure S6) and could be related to already observed ecotypes of Mediterranean  
361 *Synechococcus* (77)□. Third, in protists, two MVSs corresponding to Mamiellales (6\_5\_14 and  
362 9\_500\_10) are respectively located in *Tara* stations where *Bathycoccus prasinos* and *Bathycoccus spp.*  
363 *TOSAG39-1* were the most abundant (Supplementary Table S2) in a previous study using *Tara* Oceans  
364 metagenomic dataset (78)□. Finally, copepods formed the largest group retrieved by metaVaR, with a  
365 predominance of calanoid species compared to cyclopoid species. Finding a high number of these species  
366 was expected, considering copepods are very abundant in oceans (79,80) and well represented in the *Tara*  
367 Oceans dataset (51).

368 Together, these MVSs show the ability of metaVaR and our taxonomic assignation to distinguish closely-  
369 related species or ecotypes, and the accuracy to retrieve species.

### 370 **Differentiation of plankton populations from a global view**

371 Our results showed clear patterns of differentiation among MVSs that depend on the basins and the size of  
372 organisms. Populations belonging to different basins tend to be more differentiated than populations



373 located in the same basins, which could be explained by relatively smaller connections within basins than  
374 between basins. While this trend has been observed several times (28,81,82)□, it hides interesting  
375 patterns. We observed the central place of NAO, relatively well connected to both MED and SAO, and a  
376 slightly lower connection between MED and SAO. Also, the SO was characterized by a relative isolation  
377 from the other basins. Indeed, SO shares few MVSs with other basins, and the latter are relatively highly  
378 differentiated. This situation was already observed notably in the copepod *Metridia lucens* (83)□, with  
379 important differences between the populations of the basin. This area is characterized by differences in  
380 environmental conditions among it, and compared to the rest of the basins, with higher silicate, nitrate and  
381 phosphate concentrations on one hand, and lower salinity and temperature on the other hand (Figure 4B,  
382 Supplementary Figure S3). Plus, water masses are driven over thousands of kilometres by the complex  
383 Antarctic Circumpolar Current (ACC) (84)□, which could favour gene flow between long-range locations  
384 all around the Antarctic. In addition, the Lagrangian data clearly traced the northward Malvinas current  
385 (an ACC branch), which mixes hot waters from the Brazil current with cold waters of the ACC in the  
386 Brazil–Malvinas Confluence(85)□, possibly favouring the isolation of species in the south of this area.  
387 This situation could explain why these MVSs are both specific to Austral *Tara* stations and highly  
388 differentiated.

389 We showed that smaller organisms, like protists and bacteria, are more structured throughout oceans than  
390 zooplankton. These groups are not characterized by the same range of population sizes, dispersal  
391 capacities nor generation times, leading to different effects on their evolution. Finally, we were able to see  
392 a unique diversity of population differentiation among MVSs (Figure 3E), from unstructured to highly  
393 differentiated MVSs. The latter observation could be understood as the capacity of MVSs to capture  
394 complexes of closely-related species, as already described, for example, in *Oithona similis* in the NAO,  
395 SAO, SO and Arctic Ocean (86).

396 However, limitations arise from the use of  $F_{ST}$ , which is affected by population effective size, described as  
397 high in plankton organisms in the few studies that estimated this parameter (13,87,88).

### 398 **Lagrangian travel times to estimate marine current transport**

399 From the computation of Lagrangian travel times and sampling sites clustering, we were first able to  
400 distinguish three basins: NAO, MED and SAO-SO. Interestingly, the isolation of SO is not observed here,  
401 reinforcing our previous observations of genetic specificities linked to the unique environmental  
402 conditions of this basin. However, important differences were also observed between and among basins.  
403 For example, the Eastern part of the SAO presented an important connection with the NAO, which reflects  
404 the North Equatorial Current that linked these locations. Moreover, we saw how travel times from the SO  
405 to the Eastern part of the SAO were relatively small, which we can be linked to the Antarctic Circumpolar  
406 Current. Inside NAO, travel times between *Tara* oceans sampling sites presented a clear West-East trend,  
407 with some local divergences, which is related to the Gulf Stream and the North Atlantic Drift. Finally,  
408 inside MED, we clearly observed a West-East trend, with three different patterns: TARA\_7/9/11 in the  
409 Western basin, TARA\_18 to 26 in the Eastern basin, and the relative isolation of TARA\_30 in the  
410 Levantine part of MED. Finally, the Haptophyta MVS from SO presented a differentiation linked to both  
411 the ACC and the Malvinas Current with the populations of TARA\_83 and TARA\_82 being highly  
412 connected by the fast Malvinas Current and a progressive eastward increase of  $F_{ST}$  from TARA\_83,  
413 TARA\_84 and TARA\_85.

414 Altogether, these results show the accuracy of this computation to reflect some of the main surface marine  
415 currents and the connectivity between *Tara* stations.

### 416 **Shaping of genomic differentiation by marine currents and environmental factors**

417 In this study, the genomic differentiation of planktonic species was partially linked to environmental  
418 parameters and Lagrangian travel times. We first saw that globally, marine currents, salinity and  
419 temperature were the most important tested drivers of genomic differentiation, and that nitrate, silicate and  
420 phosphate had a relatively lower impact and this does not seem to be clade specific. Salinity and  
421 temperature are known to affect biogeography, community composition and population structure  
422 (15,28,43,49,89)□. The role of nutrients like nitrate (90)□, silicate (25,91,92)□ and phosphate (93)□ in

423 marine micro-organisms metabolism, diversity and in the frame of their biogeochemical cycles (94–96)  
424 has been well studied, but their impact on the population structure has never been investigated at this  
425 scale.

426 This study also points to the importance of computing Lagrangian travel time estimates to evaluate the  
427 role of transport by marine currents, that is critical for the understanding of plankton genomic  
428 differentiation, as underlined here and in previous studies (34,36,40,97). We can note that obtaining  
429 proper haplotypes or genotypes together with considering the asymmetric travel times between locations  
430 would allow measuring the directional gene flow between populations.

431 We also notice that a large part of genomic differentiation cannot be explained in this study. The absence  
432 of physico-chemical parameters like metals, a key for cellular metabolism (19,98), sulfur (99) or pH  
433 (18) could also enhance our comprehension of plankton genomic differentiation. Also, the contribution of  
434 biotic interactions between trophic levels, like grazing on phytoplankton by zooplankton (100) should  
435 also be examined.

#### 436 **Plankton connectivity as a mosaic**

437 Finally, in our study, the identification of group of planktonic species having similar genomic  
438 differentiation trends driven by abiotic factors clearly demonstrated the mosaic of plankton population  
439 differentiation. This mosaic trend is underlined by the diversity of environmental conditions influencing  
440 the differentiation but was also exemplified by the absence of link between the number of basins where  
441 MVSs were detected and their global differentiation (Figure 3F) and with several individual cases. This  
442 shows that the living range of species is not correlated to their population structure, i.e. cosmopolitan  
443 species do not necessarily present an absence of population structure and species with populations present  
444 in close locations can exhibit high differentiation (such as SO). We thus showed how population genomics  
445 is important to decipher the connectivity of plankton, and can be complementary to the traditional  
446 metabarcoding approach, that fails to quantify the connectivity and intra-species structure patterns.

447 Furthermore, we showed that the clade of species was not determinant to identify the drivers of the  
448 genomic differentiation.

449 The next step would be to better catch the relative effects of evolutive forces on genome, like genetic drift  
450 and selection, as the question is still unresolved (13,15–17)□. Sequencing genomes or haplotypes data  
451 could resolve this question, but in the frame of metagenomic, the latter is still a technical and  
452 computational challenge.

## 453 **Acknowledgments**

454 We thank the Commissariat à l’Energie Atomique et aux énergies alternatives, France Génomique (ANR-  
455 10-INBS-09), and Oceanomics (ANR-11-BTBR-0008). We acknowledge Paul Frémont for his help with  
456 WOA environmental parameters. This is contribution number XX from *Tara Oceans*.

## 457 **Author’s contributions**

458 RLJ performed all analyses. MAM designed and supervised the study. CA gave expertise support on the  
459 statistical framework. MO computed Lagrangian travel time estimates and MO and AS offered expertise  
460 on these results. PW offered scientific support.

## 461 **Data availability**

462 The set of MVSs is available on github at: <https://github.com/rlassojad/Metavariant-Species>

## 463 **Competing interests**

464 The authors declare no competing interests.

## 465 **References**

- 466 1. Longhurst AR, Glen Harrison W. The biological pump: Profiles of plankton production and  
467 consumption in the upper ocean. *Prog Oceanogr.* 1989;22(1):47–123.
- 468 2. Steinberg DK, Landry MR. Zooplankton and the Ocean Carbon Cycle. *Ann Rev Mar Sci.*  
469 2017;9(1):413–44.
- 470 3. Wassmann P, Reigstad M, Haug T, Rudels B, Carroll ML, Hop H, et al. Food webs and carbon  
471 flux in the Barents Sea. *Prog Oceanogr.* 2006;71(2–4):232–87.
- 472 4. Lima-Mendez G, Faust K, Henry N, Decelle J, Colin S, Carcillo F, et al. Determinants of  
473 community structure in the global plankton interactome. *Science (80- )* [Internet].  
474 2015;10(6237):1–10. Available from: [www.sciencemag.org](http://www.sciencemag.org)
- 475 5. Bucklin A, Ortman BD, Jennings RM, Nigro LM, Sweetman CJ, Copley NJ, et al. A “Rosetta  
476 Stone” for metazoan zooplankton: DNA barcode analysis of species diversity of the Sargasso Sea  
477 (Northwest Atlantic Ocean). *Deep Res Part II Top Stud Oceanogr* [Internet]. 2010;57(24–  
478 26):2234–47. Available from: <http://dx.doi.org/10.1016/j.dsr2.2010.09.025>
- 479 6. Malviya S, Scalco E, Audic S, Vincent F, Veluchamy A, Poulain J, et al. Insights into global  
480 diatom distribution and diversity in the world’s ocean. *Proc Natl Acad Sci U S A.*  
481 2016;113(11):1516–25.
- 482 7. Pierella Karlusich JJ, Ibarbalz FM, Bowler C. Phytoplankton in the Tara Ocean. *Ann Rev Mar Sci.*  
483 2020;233–65.
- 484 8. Worm B, Barbier EB, Beaumont N, Duffy JE, Folke C, Halpern BS, et al. Impacts of biodiversity  
485 loss on ocean ecosystem services. *Science (80- )*. 2006;314(5800):787–90.
- 486 9. Smith ADM, Brown CJ, Bulman CM, Fulton EA, Johnson P, Kaplan IC, et al. Impacts of fishing  
487 low-trophic level species on marine ecosystems. *Science (80- )*. 2011;333(6046):1147–50.
- 488 10. Beaugrand G. Reorganization of North Atlantic Marine Copepod Biodiversity and Climate.  
489 *Science (80- )* [Internet]. 2002;296(5573):1692–4. Available from:  
490 <http://www.sciencemag.org/cgi/doi/10.1126/science.1071329>
- 491 11. Guinder VA, Molinero JC. Climate change effects on marine phytoplankton. *Mar Ecol a Chang*  
492 *World.* 2013;(October):68–90.
- 493 12. Norris RD. Pelagic species diversity, biogeography, and evolution. *Paleobiology.* 2000;26:236–58.
- 494 13. Peijnenburg KTCA, Goetze E. High evolutionary potential of marine zooplankton. *Ecol Evol*  
495 [Internet]. 2013;3(8):2765–81. Available from: <http://doi.wiley.com/10.1002/ece3.644>
- 496 14. Collins S, Rost B, Rynearson TA. Evolutionary potential of marine phytoplankton under ocean  
497 acidification. *Evol Appl.* 2014;7(1):140–55.
- 498 15. Delmont TO, Kiefl E, Kilinc O, Esen OC, Uysal I, Rappé MS, et al. Single-amino acid variants  
499 reveal evolutionary processes that shape the biogeography of a global SAR11 subclade. *Elife.*  
500 2019;8:1–26.
- 501 16. Hellweger FL, Van Sebille E, Fredrick ND. Biogeographic patterns in ocean microbes emerge in a

- 502 neutral agent-based model. *Science* (80- ). 2014;345(6202):1346–9.
- 503 17. Ron R, Fragman-Sapir O, Kadmon R. Dispersal increases ecological selection by increasing  
504 effective community size. *Proc Natl Acad Sci U S A*. 2018;115(44):11280–5.
- 505 18. Lewis CN, Brown KA, Edwards LA, Cooper G, Findlay HS. Sensitivity to ocean acidification  
506 parallels natural pCO<sub>2</sub> gradients experienced by Arctic copepods under winter sea ice. *Proc Natl  
507 Acad Sci U S A*. 2013;110(51).
- 508 19. Mackey KRM, Post AF, McIlvin MR, Cutter GA, John SG, Saito MA, et al. Divergent responses  
509 of Atlantic coastal and oceanic *Synechococcus* to iron limitation. *Proc Natl Acad Sci U S A*.  
510 2015;112(32):9944–9.
- 511 20. Maas AE, Lawson GL, Tarrant AM. Transcriptome-wide analysis of the response of the thecosome  
512 pteropod *Clio pyramidata* to short-term CO<sub>2</sub> exposure. *Comp Biochem Physiol - Part D Genomics  
513 Proteomics* [Internet]. 2015;16:1–9. Available from: <http://dx.doi.org/10.1016/j.cbd.2015.06.002>
- 514 21. Laso-Jadart R, Sugier K, Petit E, Labadie K, Peterlongo P, Ambroise C, et al. Investigating  
515 population-scale allelic differential expression in wild populations of *Oithona similis* (Cyclopoida,  
516 Claus, 1866). *Ecol Evol*. 2020;10(16):8894–905.
- 517 22. Provan J, Beatty GE, Keating SL, Maggs CA, Savidge G. High dispersal potential has maintained  
518 long-term population stability in the North Atlantic copepod *Calanus finmarchicus*. *Proc R Soc B  
519 Biol Sci*. 2009;276(1655):301–7.
- 520 23. Kozol R, Blanco-Bercial L, Bucklin A. Multi-Gene Analysis Reveals a Lack of Genetic  
521 Divergence between *Calanus agulhensis* and *C. sinicus* (Copepoda; Calanoida). *PLoS One*.  
522 2012;7(10).
- 523 24. Weydmann A, Coelho NC, Serrão EA, Burzyński A, Pearson GA. Pan-Arctic population of the  
524 keystone copepod *Calanus glacialis*. *Polar Biol*. 2016;39(12):2311–8.
- 525 25. Biard T, Bigeard E, Audic S, Poulain J, Gutierrez-Rodriguez A, Pesant S, et al. Biogeography and  
526 diversity of *Collodaria* (Radiolaria) in the global ocean. *ISME J* [Internet]. 2017;11(6):1331–44.  
527 Available from: <http://dx.doi.org/10.1038/ismej.2017.12>
- 528 26. Stopar K, Ramšak A, Trontelj P, Malej A. Lack of genetic structure in the jellyfish *Pelagia  
529 noctiluca* (Cnidaria: Scyphozoa: Semaestomeae) across European seas. *Mol Phylogenet Evol*  
530 [Internet]. 2010;57(1):417–28. Available from: <http://dx.doi.org/10.1016/j.ympev.2010.07.004>
- 531 27. Goetze E. Population differentiation in the open sea: Insights from the pelagic copepod  
532 *pleuromamma xiphias*. *Integr Comp Biol*. 2011;51(4):580–97.
- 533 28. Burrige AK, Goetze E, Raes N, Huisman J, Peijnenburg KTCA. Global biogeography and  
534 evolution of *Cuvierina* pteropods Phylogenetics and phylogeography. *BMC Evol Biol* [Internet].  
535 2015;15(1):1–16. Available from: ???
- 536 29. Casteleyn G, Leliaert F, Backeljau T, Debeer AE, Kotaki Y, Rhodes L, et al. Limits to gene flow in  
537 a cosmopolitan marine planktonic diatom. *Proc Natl Acad Sci U S A*. 2010;107(29):12952–7.
- 538 30. Werner S, Gerhard J, Bruno S, Bernd S. Speciation and phylogeography in the cosmopolitan  
539 marine moon jelly, *Aurelia* sp. *BMC Evol Biol* [Internet]. 2002;2(1). Available from:  
540 <http://www.doaj.org/doaj?func=openurl&issn=14712148&date=2002&volume=2&issue=1&spage=1&genre=article>  
541

- 542 31. Peijnenburg KTCA, Fauvelot C, Breeuwer JAJ, Menken SBJ. Spatial and temporal genetic  
543 structure of the planktonic *Sagitta setosa* (Chaetognatha) in European seas as revealed by  
544 mitochondrial and nuclear DNA markers. *Mol Ecol*. 2006;15(11):3319–38.
- 545 32. Edmands S. Phylogeography of the intertidal copepod *Tigriopus californicus* reveals substantially  
546 reduced population differentiation at northern latitudes. *Mol Ecol*. 2001;10(7):1743–50.
- 547 33. Yebra L, Bonnet D, Harris RP, Lindeque PK, Peijnenburg KTCA. Barriers in the pelagic:  
548 Population structuring of *Calanus helgolandicus* and *C. euxinus* in European waters. *Mar Ecol*  
549 *Prog Ser*. 2011;428:135–49.
- 550 34. Madoui MA, Poulain J, Sugier K, Wessner M, Noel B, Berline L, et al. New insights into global  
551 biogeography, population structure and natural selection from the genome of the epipelagic  
552 copepod *Oithona*. *Mol Ecol*. 2017;26(17):4467–82.
- 553 35. Richlen ML, Erdner DL, McCauley LAR, Liberal K, Anderson DM. Extensive genetic diversity  
554 and rapid population differentiation during blooms of *Alexandrium fundyense* (dinophyceae) in an  
555 isolated salt pond on cape cod, MA, USA. *Ecol Evol*. 2012;2(10):2588–99.
- 556 36. Alberto F, Raimondi PT, Reed DC, Watson JR, Siegel DA, Mitarai S, et al. Isolation by  
557 oceanographic distance explains genetic structure for *Macrocystis pyrifera* in the Santa Barbara  
558 Channel. *Mol Ecol*. 2011;20(12):2543–54.
- 559 37. Fontaine MC, Baird SJE, Piry S, Ray N, Tolley KA, Duke S, et al. Rise of oceanographic barriers  
560 in continuous populations of a cetacean: The genetic structure of harbour porpoises in Old World  
561 waters. *BMC Biol*. 2007;5:1–16.
- 562 38. Riginos C, Crandall ED, Liggins L, Bongaerts P, Trembl EA. Navigating the currents of seascape  
563 genomics: How spatial analyses can augment population genomic studies. *Curr Zool*.  
564 2016;62(6):581–601.
- 565 39. Galindo HM, Pfeiffer-Herbert AS, McManus MA, Chao Y, Chai F, Palumbi SR. Seascape genetics  
566 along a steep cline: Using genetic patterns to test predictions of marine larval dispersal. *Mol Ecol*.  
567 2010;19(17):3692–707.
- 568 40. Dalongeville A, Andrello M, Mouillot D, Lobreaux S, Fortin M-J, Lasram F, et al. Geographic  
569 isolation and larval dispersal shape seascape genetic patterns differently according to spatial scale.  
570 *Evol Appl* [Internet]. 2018;11(December 2017):1437–47. Available from:  
571 <http://doi.wiley.com/10.1111/eva.12638>
- 572 41. Riginos C, Hock K, Matias AM, Mumby PJ, van Oppen MJH, Lukoschek V. Asymmetric dispersal  
573 is a critical element of concordance between biophysical dispersal models and spatial genetic  
574 structure in Great Barrier Reef corals. *Divers Distrib*. 2019;25(11):1684–96.
- 575 42. Sjöqvist C, Godhe A, Jonsson PR, Sundqvist L, Kremp A. Local adaptation and oceanographic  
576 connectivity patterns explain genetic differentiation of a marine diatom across the North Sea-Baltic  
577 Sea salinity gradient. *Mol Ecol*. 2015;24(11):2871–85.
- 578 43. Ueda H, Yamaguchi A, Saitoh S ichi, Sakaguchi SO, Tachihara K. Speciation of two salinity-  
579 associated size forms of *Oithona dissimilis* (Copepoda: Cyclopoida) in estuaries. *J Nat Hist*.  
580 2011;45(33–34):2069–79.
- 581 44. Smetacek V. Making sense of ocean biota: How evolution and biodiversity of land organisms  
582 differ from that of the plankton. *J Biosci*. 2012;37(4):589–607.

- 583 45. Bucklin A, DiVito KR, Smolina I, Choquet M, Questel JM, Hoarau G, et al. Population Genomics  
584 of Marine Zooplankton. In: Population Genomics: Marine Organisms. Springer; 2018. p. 0–66.
- 585 46. Yooseph S, Sutton G, Rusch DB, Halpern AL, Williamson SJ, Remington K, et al. The Sorcerer II  
586 global ocean sampling expedition: Expanding the universe of protein families. PLoS Biol.  
587 2007;5(3):0432–66.
- 588 47. Karsenti E, Acinas SG, Bork P, Bowler C, De Vargas C, Raes J, et al. A Holistic Approach to  
589 Marine Eco-Systems Biology. PLoS Biol [Internet]. 2011 Oct 18;9(10). Available from:  
590 <https://dx.plos.org/10.1371/journal.pbio.1001177>
- 591 48. Brum JR, Ignacio-espinoza JC, Roux S, Doucier G, Acinas SG, Alberti A, et al. Ocean Viral  
592 Communities. Science (80- ). 2015;348(6237):1261498-1–11.
- 593 49. Sunagawa S, Coelho LP, Chaffron S, Kultima JR, Labadie K, Salazar G, et al. Structure and  
594 function of the global ocean microbiome. Science (80- ). 2015;348(6237):1–10.
- 595 50. Carradec Q, Pelletier E, Da Silva C, Alberti A, Seeleuthner Y, Blanc-Mathieu R, et al. A global  
596 ocean atlas of eukaryotic genes. Nat Commun [Internet]. 2018 Dec 25;9(1):373. Available from:  
597 <http://www.nature.com/articles/s41467-017-02342-1>
- 598 51. Vorobev A, Dupouy M, Carradec Q, Delmont TO, Annamali A, Wincker P, et al. Transcriptome  
599 reconstruction and functional analysis of eukaryotic marine plankton communities via high-  
600 throughput metagenomics and metatranscriptomics. Genome Res. 2020;30(4):647–59.
- 601 52. Parks DH, Rinke C, Chuvochina M, Chaumeil PA, Woodcroft BJ, Evans PN, et al. Recovery of  
602 nearly 8,000 metagenome-assembled genomes substantially expands the tree of life. Nat Microbiol  
603 [Internet]. 2017;2(11):1533–42. Available from: <http://dx.doi.org/10.1038/s41564-017-0012-7>
- 604 53. Delmont TO, Quince C, Shaiber A, Esen ÖC, Lee ST, Rappé MS, et al. Nitrogen-fixing  
605 populations of Planctomycetes and Proteobacteria are abundant in surface ocean metagenomes. Nat  
606 Microbiol. 2018;3(7):804–13.
- 607 54. Stewart RD, Auffret MD, Warr A. et al. Assembly of 913 microbial genomes from metagenomic  
608 sequencing of the cow rumen. Nat Commun. 2018;9(870).
- 609 55. Delmont TO, Gaia M, Hinsinger DD, Fremont P, Fernandez Guerra A, Murat Eren A, et al.  
610 Functional repertoire convergence of distantly related eukaryotic plankton lineages revealed by  
611 genome-resolved metagenomics. BioRxiv [Internet]. 2020;2020.10.15.341214. Available from:  
612 <https://doi.org/10.1101/2020.10.15.341214>
- 613 56. Seeleuthner Y, Mondy S, Lombard V, Carradec Q, Pelletier E, Wessner M, et al. Single-cell  
614 genomics of multiple uncultured stramenopiles reveals underestimated functional diversity across  
615 oceans. Nat Commun. 2018;9(1):1–10.
- 616 57. Laso-Jadart R, Ambroise C, Peterlongo P, Madoui MA. MetaVaR: Introducing metavariant species  
617 models for reference-free metagenomic-based population genomics. PLoS One [Internet]. 2020;1–  
618 17. Available from: <http://dx.doi.org/10.1371/journal.pone.0244637>
- 619 58. O'Malley M, Sykulski AM, Laso-Jadart R, Madoui M-A. Estimating the travel time and the most  
620 likely path from Lagrangian drifters. arXiv [Internet]. 2020;1–24. Available from:  
621 <http://arxiv.org/abs/2002.07774>
- 622 59. Peterlongo P, Riou C, Drezen E, Lemaitre C. DiscoSnp++: de novo detection of small variants



- 623 from raw unassembled read set(s). bioRxiv [Internet]. 2017;209965. Available from:  
624 <https://www.biorxiv.org/content/early/2017/10/27/209965>
- 625 60. Arif M, Gauthier J, Sugier K, Iudicone D, Jaillon O, Wincker P, et al. Discovering Millions of  
626 Plankton Genomic Markers from the Atlantic Ocean and the Mediterranean Sea. *Mol Eco Res*.  
627 2019;19(2):526–35.
- 628 61. Pesant S, Not F, Picheral M, Kandels-Lewis S, Le Bescot N, Gorsky G, et al. Open science  
629 resources for the discovery and analysis of Tara Oceans data. *Sci Data* [Internet]. 2015 Dec  
630 26;2(1). Available from: <http://www.nature.com/articles/sdata201523>
- 631 62. Alberti A, Poulain J, Engelen S, Labadie K, Romac S, Ferrera I, et al. Viral to metazoan marine  
632 plankton nucleotide sequences from the Tara Oceans expedition. *Sci Data* [Internet]. 2017 Aug 1  
633 [cited 2019 Jan 7];4:170093. Available from: <http://www.nature.com/articles/sdata201793>
- 634 63. Ester M, Kriegel H-P, Sander J, Xu X. A Density-Based Algorithm for Discovering Clusters in  
635 Large Spatial Databases with Noise [Internet]. 1996 [cited 2019 Jan 8]. Available from:  
636 [www.aaai.org](http://www.aaai.org)
- 637 64. Ram A, Jalal S, Jalal AS, Kumar M. A Density Based Algorithm for Discovering Density Varied  
638 Clusters in Large Spatial Databases. *Int J Comput Appl* [Internet]. 2010;3(6):1–4. Available from:  
639 <http://www.ijcaonline.org/volume3/number6/pxc3871038.pdf>
- 640 65. Buchfink B, Xie C, Huson DH. Fast and sensitive protein alignment using DIAMOND. *Nat*  
641 *Methods*. 2014;12(1):59–60.
- 642 66. Genoscope. Fuzzy LCA [Internet]. 2018. Available from: <https://github.com/institut-de-genomique/fuzzy-lca-module>
- 644 67. Keeling PJ, Burki F, Wilcox HM, Allam B, Allen EE, Amaral-Zettler LA, et al. The Marine  
645 Microbial Eukaryote Transcriptome Sequencing Project (MMETSP): Illuminating the Functional  
646 Diversity of Eukaryotic Life in the Oceans through Transcriptome Sequencing. *PLoS Biol*.  
647 2014;12(6).
- 648 68. Weir BS, Cockerham CC. Estimating F-Statistics for the Analysis of Population Structure.  
649 *Evolution* (N Y). 1984;38(6):1358–70.
- 650 69. Wu P, Haines K. Modeling the dispersal of Levantine Intermediate Water and its role in  
651 Mediterranean deep water formation. *J Geophys Res C Ocean*. 1996;101(C3):6591–607.
- 652 70. El-Geziry TM, Bryden IG. The circulation pattern in the Mediterranean Sea: Issues for modeller  
653 consideration. *J Oper Oceanogr*. 2010;3(2):39–46.
- 654 71. Laporte F, Mary-Huard T. MM4LMM: Inference of Linear Mixed Models Through MM  
655 Algorithm [Internet]. 2019. Available from: <https://cran.r-project.org/package=MM4LMM>
- 656 72. Lê S, Josse J, Husson F. FactoMineR: An R Package for Multivariate Analysis. *J Stat Softw*  
657 [Internet]. 2008;25(1):1–18. Available from: <http://www.jstatsoft.org/v25/i01>
- 658 73. Husson F, Josse J, Lê S, Mazet J. FactoMineR: Multivariate Exploratory Data Analysis and Data  
659 Mining [Internet]. 2020. Available from: <https://cran.r-project.org/package=FactoMineR>
- 660 74. Krijthe J, Van der Maaten L. Rtsne: T-Distributed Stochastic Neighbor Embedding using a Barnes-  
661 Hut Implementation [Internet]. 2018. Available from: <https://cran.r-project.org/package=Rtsne>

- 662 75. Sullivan MB, Huang KH, Ignacio-Espinoza JC, Berlin AM, Kelly L, Weigele PR, et al. Genomic  
663 analysis of oceanic cyanobacterial myoviruses compared with T4-like myoviruses from diverse  
664 hosts and environments. *Environ Microbiol.* 2010;12(11):3035–56.
- 665 76. Gregory AC, Zayed AA, Conceição-Neto N, Temperton B, Bolduc B, Alberti A, et al. Marine  
666 DNA Viral Macro- and Microdiversity from Pole to Pole. *Cell.* 2019;177(5):1109–23.
- 667 77. Mella-Flores D, Mazard S, Humily F, Partensky F, Mahé F, Bariat L, et al. Is the distribution of  
668 *Prochlorococcus* and *Synechococcus* ecotypes in the Mediterranean Sea affected by global  
669 warming? *Biogeosciences.* 2011;8(9):2785–804.
- 670 78. Leconte J, Benites LF, Vannier T, Wincker P, Piganeau G, Jaillon O. Genome resolved  
671 biogeography of mamiellales. *Genes (Basel).* 2020;11(1).
- 672 79. Humes AG. How Many Copepods? *Hydrobiologia.* 1994;293(1951):1–7.
- 673 80. Gallienne CP. Is *Oithona* the most important copepod in the world’s oceans? *J Plankton Res*  
674 [Internet]. 2001;23(12):1421–32. Available from: [https://academic.oup.com/plankt/article-](https://academic.oup.com/plankt/article-lookup/doi/10.1093/plankt/23.12.1421)  
675 [lookup/doi/10.1093/plankt/23.12.1421](https://academic.oup.com/plankt/article-lookup/doi/10.1093/plankt/23.12.1421)
- 676 81. Kulagin DN, Stupnikova AN, Neretina T V., Muge NS. Spatial genetic heterogeneity of the  
677 cosmopolitan chaetognath *Eukrohnia hamata* (Möbius, 1875) revealed by mitochondrial DNA.  
678 *Hydrobiologia.* 2014;721(1):197–207.
- 679 82. Hirai J, Tsuda A, Goetze E. Extensive genetic diversity and endemism across the global range of  
680 the oceanic copepod *Pleuromamma abdominalis*. *Prog Oceanogr* [Internet]. 2015;138:77–90.  
681 Available from: <http://dx.doi.org/10.1016/j.pocean.2015.09.002>
- 682 83. Stupnikova AN, Molodtsova TN, Muge NS, Neretina T V. Genetic variability of the *Metridia*  
683 *lucens* complex (Copepoda) in the Southern Ocean. *J Mar Syst* [Internet]. 2013 Dec;128:175–84.  
684 Available from: <http://dx.doi.org/10.1016/j.jmarsys.2013.04.016>
- 685 84. Sokolov S, Rintoul SR. Circumpolar structure and distribution of the antarctic circumpolar current  
686 fronts: 1. Mean circumpolar paths. *J Geophys Res Ocean.* 2009;114(11):1–19.
- 687 85. Goni G, Kamholz S, Garzoli S, Olson D. Dynamics of the Brazil-Malvinas confluence based on  
688 inverted echo sounders and altimetry. *J Geophys Res.* 1996;101(C7):16273–89.
- 689 86. Cornils A, Wend-Heckmann B, Held C. Global phylogeography of *Oithona similis* s.l. (Crustacea,  
690 Copepoda, Oithonidae) – A cosmopolitan plankton species or a complex of cryptic lineages? *Mol*  
691 *Phylogenet Evol* [Internet]. 2017;107:473–85. Available from:  
692 <http://dx.doi.org/10.1016/j.ympev.2016.12.019>
- 693 87. Aarbakke ONS, Bucklin A, Halsband C, Norrbin F. Comparative phylogeography and  
694 demographic history of five sibling species of *Pseudocalanus* (Copepoda: Calanoida) in the North  
695 Atlantic Ocean. *J Exp Mar Bio Ecol* [Internet]. 2014;461:479–88. Available from:  
696 <http://dx.doi.org/10.1016/j.jembe.2014.10.006>
- 697 88. Blanc-Mathieu R, Krasovec M, Hebrard M, Yau S, Desgranges E, Martin J, et al. Population  
698 genomics of picophytoplankton unveils novel chromosome hypervariability. *Sci Adv* [Internet].  
699 2017 Jul 5;3(7). Available from:  
700 <https://advances.sciencemag.org/lookup/doi/10.1126/sciadv.1700239>
- 701 89. Castellani C, Licandro P, Fileman E, Di Capua I, Mazzocchi MG. *Oithona similis* likes it cool:

- 702 evidence from two long-term time series. *J Plankton Res.* 2016;38(October):762–70.
- 703 90. Kitzinger K, Marchant HK, Bristow LA, Herbold CW, Padilla CC, Kidane AT, et al. Single cell  
704 analyses reveal contrasting life strategies of the two main nitrifiers in the ocean. *Nat Commun*  
705 [Internet]. 2020;in press. Available from: <http://dx.doi.org/10.1038/s41467-020-14542-3>
- 706 91. Baines SB, Twining BS, Brzezinski MA, Krause JW, Vogt S, Assael D, et al. Significant silicon  
707 accumulation by marine picocyanobacteria. *Nat Geosci* [Internet]. 2012;5(12):886–91. Available  
708 from: <http://dx.doi.org/10.1038/ngeo1641>
- 709 92. Ohnemus DC, Rauschenberg S, Krause JW, Brzezinski MA, Collier JL, Geraci-Yee S, et al.  
710 Silicon content of individual cells of *Synechococcus* from the North Atlantic Ocean. *Mar Chem*  
711 [Internet]. 2016;187:16–24. Available from: <http://dx.doi.org/10.1016/j.marchem.2016.10.003>
- 712 93. Karl DM. Microbially Mediated Transformations of Phosphorus in the Sea: New Views of an Old  
713 Cycle. *Ann Rev Mar Sci.* 2014;6(1):279–337.
- 714 94. Tyrrell T. The relative influences of nitrogen and phosphorus on oceanic primary production. *III*  
715 *Med J.* 1975;148(5):551–5.
- 716 95. Levitus S, Conkright ME, Reid JL, Najjar RG, Mantyla A. Distribution of nitrate, phosphate and  
717 silicate in the world oceans. *Prog Oceanogr.* 1993;31(3):245–73.
- 718 96. Martiny AC, Lomas MW, Fu W, Boyd PW, Chen Y ling L, Cutter GA, et al. Biogeochemical  
719 controls of surface ocean phosphate. *Sci Adv.* 2019;5(8):1–10.
- 720 97. Sala I, Caldeira RMA, Estrada-Allis SN, Froufe E, Couvelard X. Lagrangian transport pathways in  
721 the northeast Atlantic and their environmental impact. *Limnol Oceanogr Fluids Environ.*  
722 2013;3(1):40–60.
- 723 98. Hawco NJ, McIlvin MM, Bundy RM, Tagliabue A, Goepfert TJ, Moran DM, et al. Minimal cobalt  
724 metabolism in the marine cyanobacterium *Prochlorococcus*. *Proc Natl Acad Sci U S A.* 2020;12.
- 725 99. Van Mooy BAS, Rocap G, Fredricks HF, Evans CT, Devol AH. Sulfolipids dramatically decrease  
726 phosphorus demand by picocyanobacteria in oligotrophic marine environments. *Proc Natl Acad*  
727 *Sci U S A.* 2006;103(23):8607–12.
- 728 100. Sjöqvist C, Kremp A, Lindehoff E, Båmstedt U, Egardt J, Gross S, et al. Effects of Grazer  
729 Presence on Genetic Structure of a Phenotypically Diverse Diatom Population. *Microb Ecol.*  
730 2014;67(1):83–95.

731

## 732 **Supplementary Tables**

733 **Supplementary Table S1: Summary of MVSs**

734 **Supplementary Table S2: MVSs and *Bathycoccus***

## 735 **Figures**

736 **Figure 1: Construction of metavariant species from metagenomic dataset of Tara Oceans.** A)  
737 Worldmap showing the locations of the 35 Tara Oceans stations used in the study. Each circle is divided  
738 in four, depending on the detection of an MVS. In grey, no MVSs were retrieved. B) Pipeline of MVS  
739 construction, with additional statistics by size fraction. From top to bottom: number of metavariants before  
740 and after filtering, number of metavariant clusters (MVC) detected and number of metavariant species  
741 (MVS) finally selected.

742 **Figure 2: Description of the set of MVSs.** A) Distribution of the number of metavariants for each size  
743 fraction. On the top, pie charts representing the taxonomic composition of each size fractions. B) Number  
744 of MVSs assigned to the six wider taxonomic groups. C) Number of MVSs according to the basins they  
745 were detected in: Northern Atlantic Ocean (NAO), SAO (Southern Atlantic Ocean), SO (Southern Ocean)  
746 and MED (Mediterranean Sea). D) World map showing the number of MVSs of each taxonomic group for  
747 each Tara station. The size of the circles corresponds to the amount of MVSs detected in each station.  
748 Colors of taxonomic groups are indicated on the bottom right of the panel.

749 **Figure 3: Global view of genomic differentiation.** A) Distributions of the 113 MVSs' pairwise- $F_{ST}$   
750 matrices. In red, pairwise- $F_{ST}$  of populations belonging to the same basin; in blue to different basins. B)  
751 Pairwise- $F_{ST}$  matrix between basins. The values represent the mean of all the median- $F_{ST}$  between stations  
752 regrouped according to the basin they belonged to. C) Distributions of the MVSs' median pairwise- $F_{ST}$ ,  
753 according to their size fractions. Black diamonds correspond to the mean of the distributions. The bars on  
754 the top correspond to the comparisons done by pairwise Wilcoxon tests (p-values: \* <0.05, \*\*<0.01,  
755 \*\*\*<0.001, \*\*\*\*<0.0001) D) Distributions of the MVSs' median pairwise- $F_{ST}$ , according to their  
756 taxonomic group. Black diamonds correspond to the mean of the distributions. Each bar corresponds to  
757 taxonomic groups displaying no significant differences. E) Scatter plot, each dot is an MVS. The size of  
758 each dot reflects the global median- $F_{ST}$  of the MVS'  $F_{ST}$  distribution (i.e.,  $F_{ST}$  computed over all the  
759 populations of an MVS). F) Global median  $F_{ST}$  compared to the number of basins MVSs were detected.  
760 Each dot is an MVS.

761 **Figure 4: Lagrangian travel times and environmental parameters.** A) Minimum times retained for  
762 analyses. In grey, asymmetric times that were not the minimum, thus the matrix accounts for the  
763 "direction" of currents between stations. B) Measures of temperature, salinity, nitrate, phosphate and  
764 silicate extracted from World Ocean Atlas (WOA) for the 35 Tara stations. On the right, color scales for  
765 each parameter. For the worldmap of Tara stations, see supplementary Figure S3.

766 **Figure 5: Variation partitioning of genomic differentiation.** A) PCA performed on the proportion of  
767 variation explained by each parameter over the 113 MVSs. The colour corresponds to the Pearson's  
768 correlation between coordinates of MVSs for a component and the variation explained by the parameters  
769 (p-values: \* <0.05, \*\*<0.01, \*\*\*<0.001, \*\*\*\*<0.0001). The size of the circles represents the relative  
770 contribution (i.e. the ratio of the variable  $\cos^2$  on the total  $\cos^2$  of the component) of each variable to each  
771 component. B) t-SNE and kmeans (K=8) clustering. Each dot represents an MVS. Each colour  
772 corresponds to a defined cluster obtained by kmeans. The names of the clusters are linked to the following  
773 figure C) Distributions of variation explained by each factor by cluster, and the taxonomic composition of  
774 each cluster. The boxplots colours are the same as the previous figure. The asterisk \* on the top of

775 boxplots corresponds to parameters that significantly contributes the most to the genomic differentiation  
776 of the MVSs included in the cluster, according to a pairwise Wilcoxon test ( $p$ -value  $< 0.05$ ).

777 **Figure 6: Examples of genomic differentiation.** A) to H) Pairwise- $F_{ST}$  matrices of MVSs mentioned in  
778 the respective titles. For each title are mentioned: the taxonomic assignation, the name, and the cluster to  
779 which the MVS belongs.

780 **Figure 7: Genomic differentiation in Southern Ocean.** A) Map localizing TARA\_82, 83, 84, 85. The  
781 two arrows correspond to the trajectories of currents, based on Lagrangian trajectories, travel times and  
782 literature B) Pairwise- $F_{ST}$  matrices of the four MVSs specific to this area.

## 783 **Supplementary Figures**

784 **Supplementary Figure S1 : MetavaR clustering**

785 **Supplementary Figure S2 : Overview of taxonomic assignation**

786 **Supplementary Figure S3 : Environmental parameters maps**

787 **Supplementary Figure S4 : Principal component analysis of the contribution of environmental**  
788 **parameters to the genomic differentiation of MVSs**

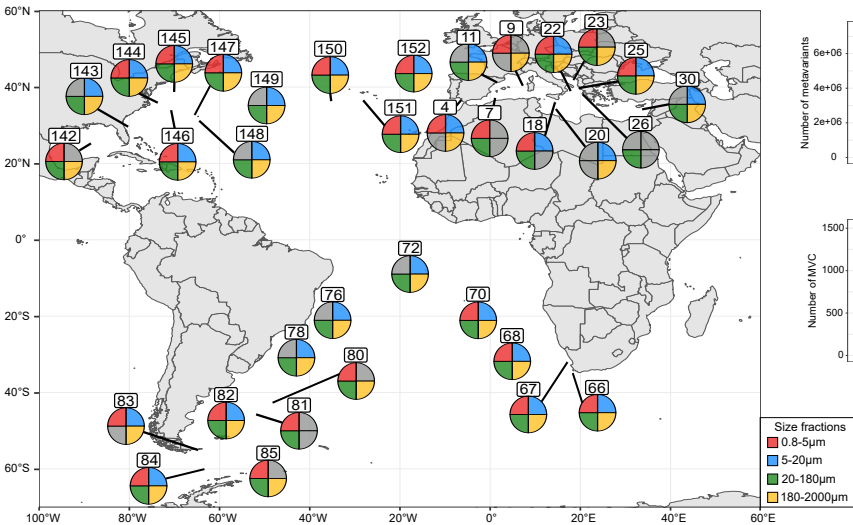
789 **Supplementary Figure S5 : Occurrence of MVSs**

790 **Supplementary Figure S6 : Global distributions of  $F_{ST}$**

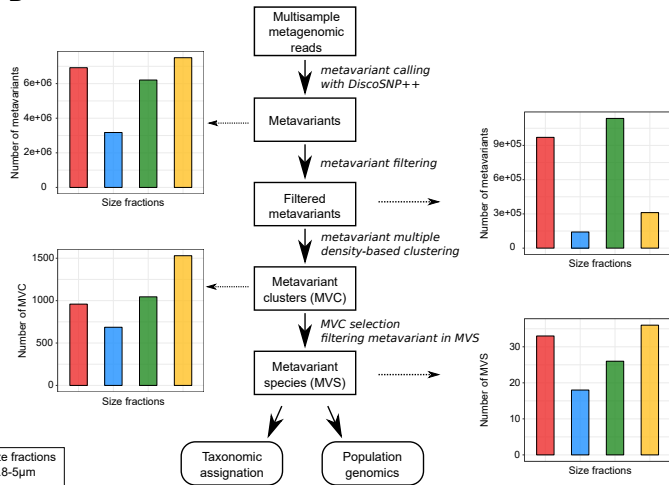
791 **Supplementary Figure S7 : Lagrangian estimates matrices**

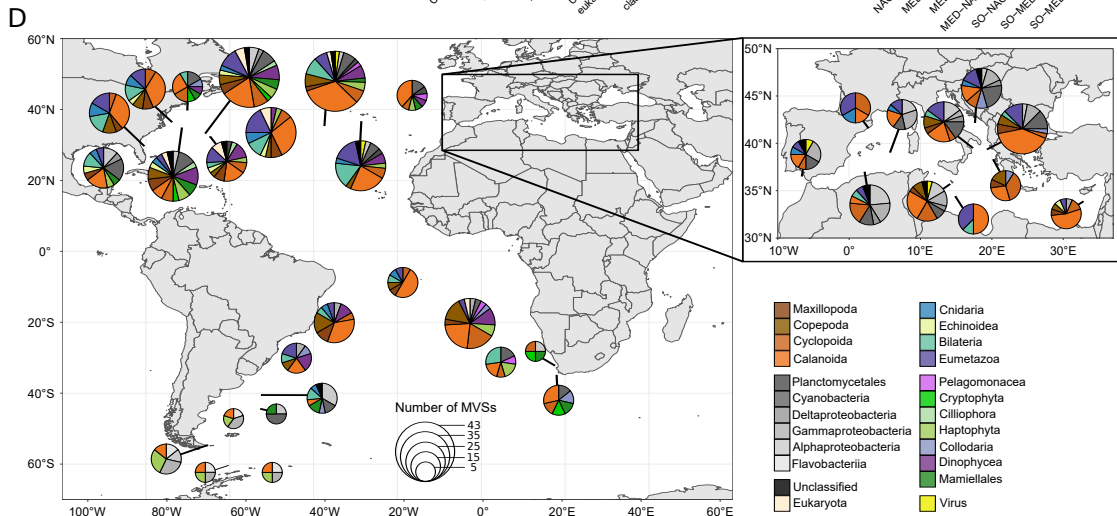
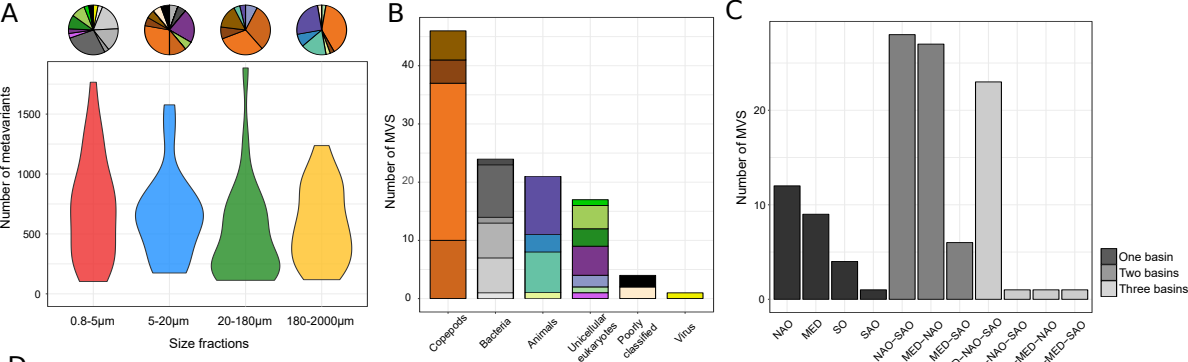
792 **Supplementary Figure S8: Lagrangian trajectories for stations of Southern Ocean.**

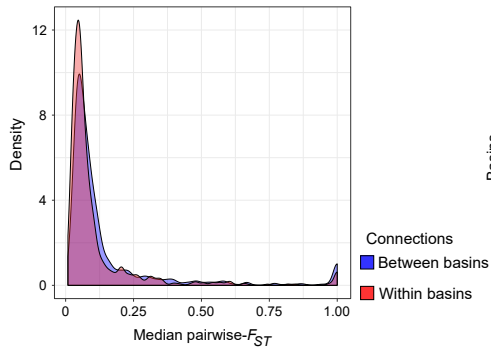
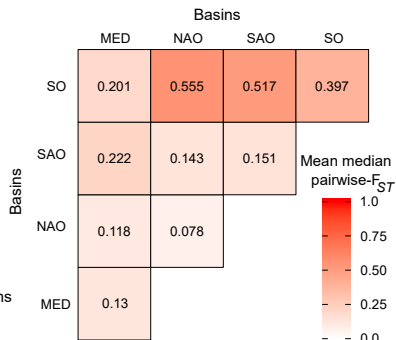
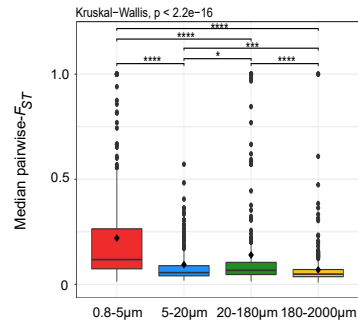
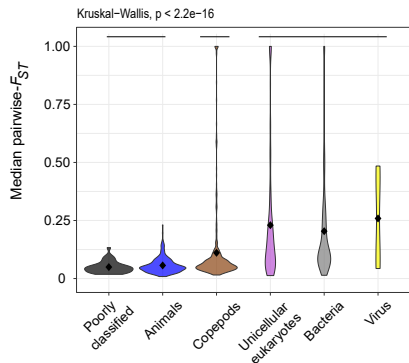
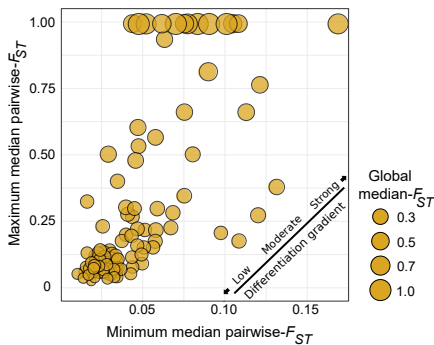
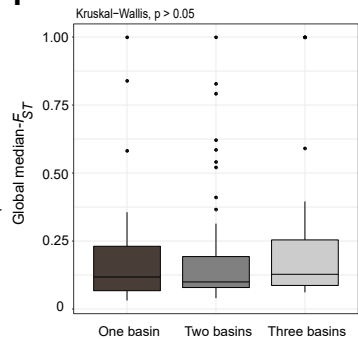
A



B

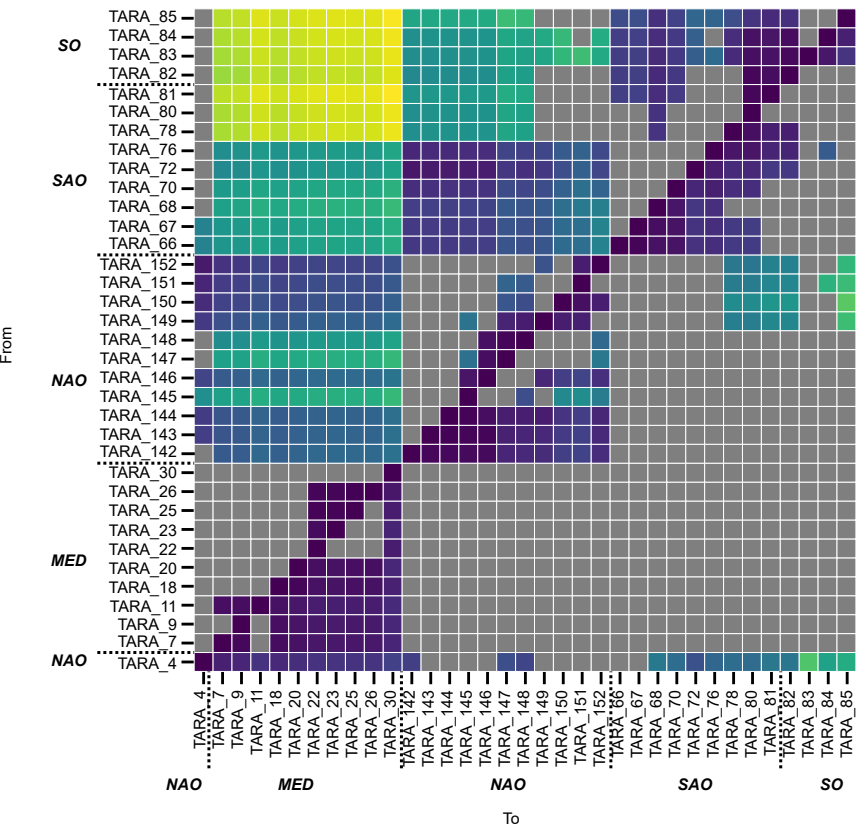




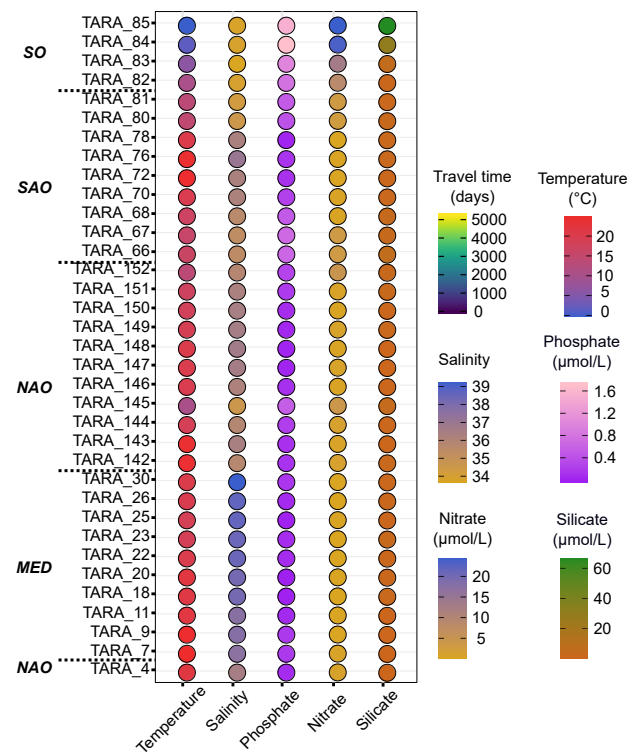
**A****B****C****D****E****F**



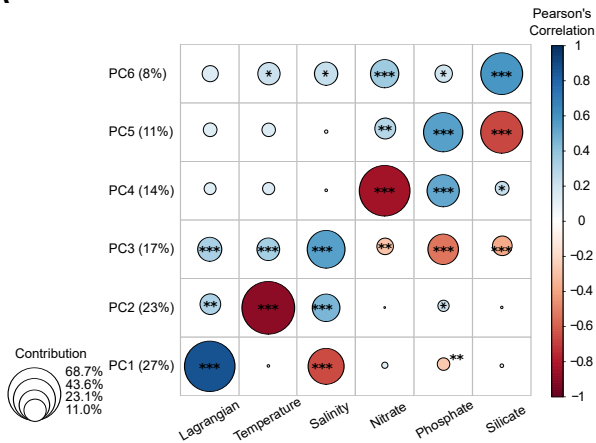
A



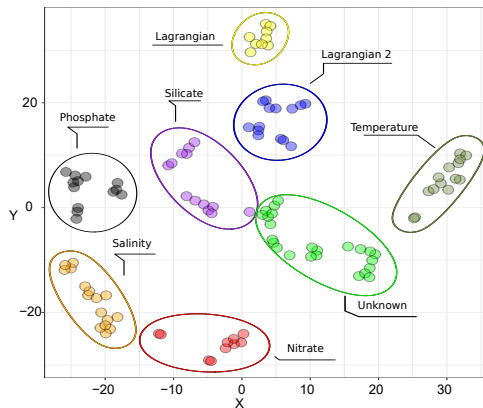
B



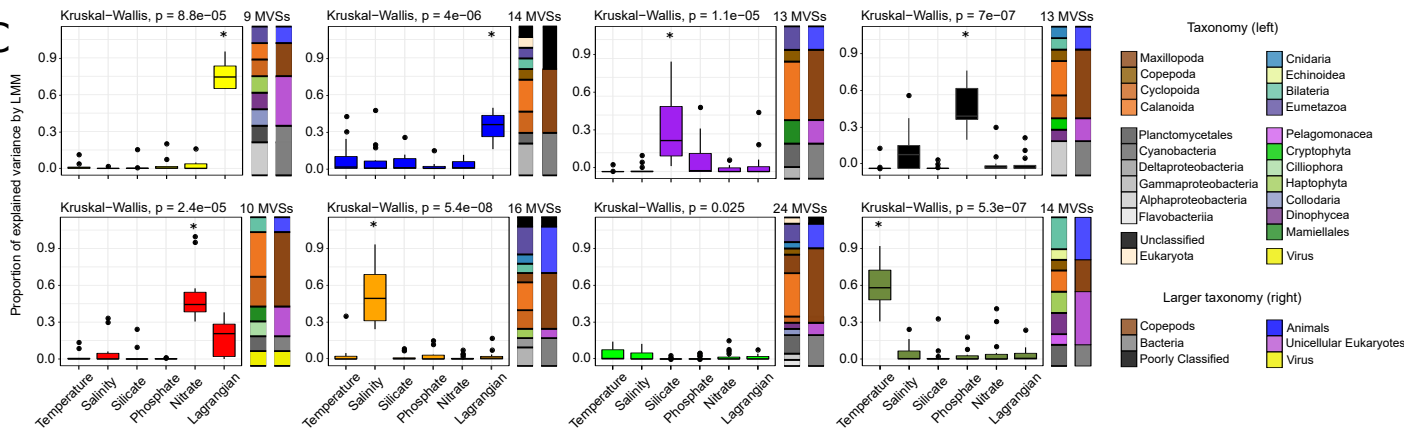
A



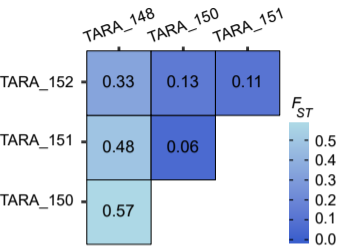
B



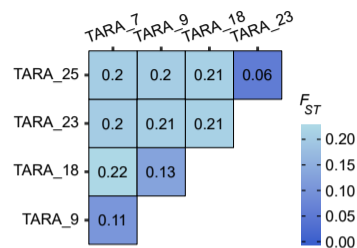
C



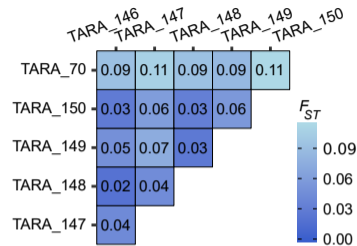
**A** Planctomycetales 9\_200\_1  
"Lagrangian"



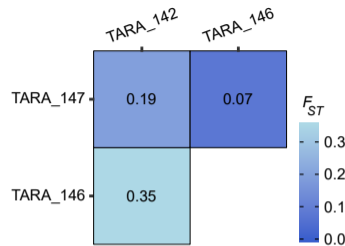
**B** Gammaproteobacteria 7\_300\_4  
"Lagrangian 2"



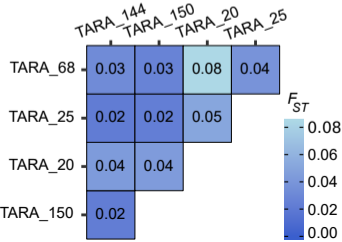
**C** Dinophyceae 8\_10\_11  
"Phosphate"



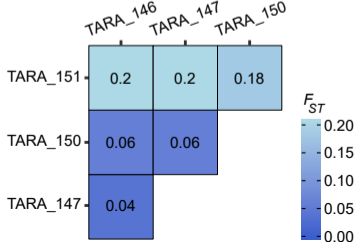
**D** Mamiellales 5\_100\_1  
"Nitrate"



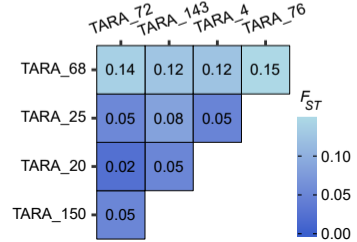
**E** Calanoida 12\_5\_104  
"Temperature"



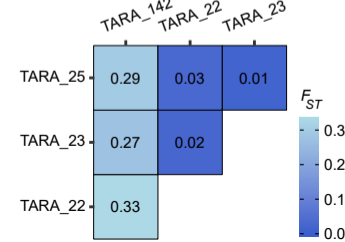
**F** Cyanobacteria 8\_100\_13  
"Silicate"



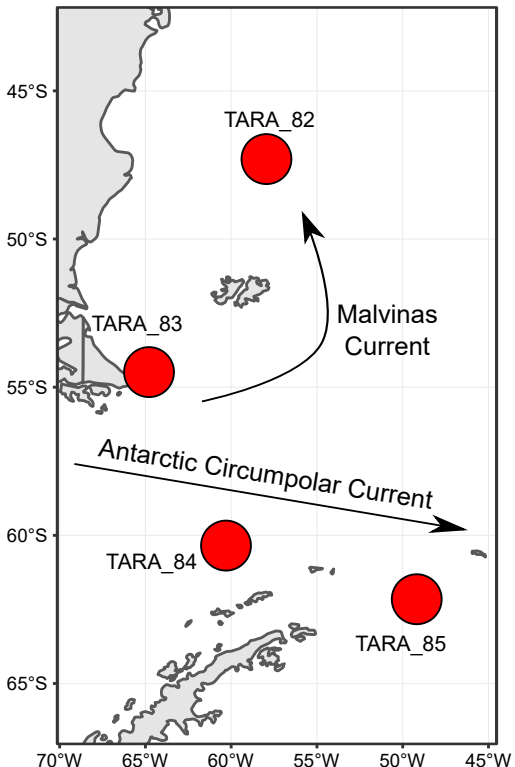
**G** Cnidaria 20\_100\_10  
"Salinity"



**H** Cyanobacteria 7\_7\_9  
"Lagrangian 2"



A



B

